Corrosion behavior of AZ31 magnesium alloy in simulated acid rain solution

LIU Feng(   ), SONG Ying-wei(   ), SHAN Da-yong(   ), HAN En-hou(   )

State Key Laboratory for Corrosion and Protection, Institute of Metal Research, Chinese Academy of Sciences,
Shenyang 110016, China

Abstract: The corrosion mechanism of AZ31 magnesium alloy used as automobile components and the influence of the concentration of Cl^- ion in simulated acid rain (SAR) were studied by electrochemical tests and SEM. The results show that pitting corrosion happens around the AlMn phases locating at the grain boundary. The corrosion of AZ31 magnesium alloy in SAR is controlled by the rate of anodic dissolution and hydrogen evolution, and the corrosion rate of AZ31 increases with increasing concentration of Cl^- ion. However, the Cl^- ion in SAR is not the main influencing factor inducing the pitting corrosion.
Key words: AZ31 magnesium alloy; simulated acid rain solution; Cl^- ion; AlMn phase

1 Introduction

Magnesium alloys have excellent application prospect in automobile industry. However, it is well known that magnesium alloys have poor corrosion resistance. It is inevitable for the corrosion of magnesium alloy components when they contact with different corrosive environment like acid rain[1−4].

Acid rain is becoming a threat to the exposed facilities, and Cl^- ion is a major corrosive element in it. The concentration of Cl^- ion is a changeable parameter which is decided by local geographic position and climatic condition. The concentration of Cl^- ion in acid rain has an important influence on the corrosion mechanism of magnesium alloys. However, most of previous studies about the influence of Cl^- ion on magnesium alloy were conducted in 3%−5% NaCl solution[3−7], but the concentration of Cl^- in acid rain was lower. The corrosion mechanism for magnesium alloy in accelerated test would be different from that in acid rain. ZHOU et al[8] studied the corrosion mechanism of the die-cast AZ91D magnesium alloy in simulated acid rain, and this alloy did present pitting corrosion. AZ31 is another kind of magnesium alloy that is used in automobile, so the influence of Cl^- ion on the corrosion behavior of AZ31 magnesium alloy in acid rain will be studied in this work.

2 Experimental

2.1 Sample preparation

The material studied was rolled AZ31 magnesium alloy. For electrochemical test, the samples were mounted by epoxide resin with 1 cm^2 surface exposed, and the surface of samples were polished using 1 000, 2 000 grit silicon carbide papers. For immersion test intending to observe the surface morphology, the samples were cut into 1 cm×1 cm×1 cm, then the surface was polished using 1 000, 2 000 grit silicon carbide papers and then finely polished using 0.5 μm diamond paste, at last samples were etched by a mixed solution containing carbazotic acid, absolute ethyl alcohol, acetic acid and water, with concentrations of 5.5 g/L, 90 mL/L, 5 mL/L and 10 mL/L, respectively. The samples were cleaned using distilled water and acetone, and then dried in cold air.

2.2 Electrochemical measurement

All the electrochemical tests and immersion tests were conducted in simulated acid rain (SAR) solution, ten times concentration of SAR solution was made up as listed in Table 1[10].

The pH value of the solution was adjusted to 4.5 using sodium hydroxide and the experiment temperature was fixed at 25 °C in this experiment. The influence of

Table.1 Concentrations of components in simulated acid rain solution

Component	Concentration/(mg·L^{-1})
Sulphuric acid (96%)	31.85
Nitric acid (70%)	15.75
Sodium nitrate	21.25
Ammonium sulfate	46.20
Sodium sulfate	31.95
Sodium chloride	84.85

the concentration of Cl$^-$ ion on the magnesium alloy was studied. Different times of concentration of Cl$^-$ SAR solution were prepared before experiment, which were 0, 1 and 2 times of concentration of Cl$^-$ in standard SAR solution and named as solution A, B, and C, correspondingly.

For electrochemical test, the ratio of sample surface to the volume of solution was 1:1 000, and SAR solution was renewed every 12 h to keep pH value constant. The samples were immerged in SAR solution for different time intervals, and then the electrochemical impendence spectroscopy (EIS) was measured using a model 5210 locked in amplifier coupled with potentiostat model 273. A conventional three electrode cell system (reference electrode is SCE) was used. The scan frequency range was 100 kHz to 10 mHz, and the perturbation amplitude was 5 mV. In the case of polarization curves test, the scan rate was 0.5 mV/s, and the scanning region was from −0.3 V to +0.4 V (vs OCP, open circuit potential). The initial retard of 300 s for all the electrochemical tests was set to obtain a stable testing system.

### 2.3 Immersion test for surface morphology observation

The samples were immerged in two kinds of solutions: solution A and solution B. The ratio of the sample surface to the volume of solution was 12:1 000. SAR solution was renewed every 12 h to keep the pH value constant. Samples were immerged in SAR solution for different time intervals. The surface morphologies were observed with Philips XL30 scanning electro microscope (SEM) equipped with energy dispersive X-ray spectroscope (EDX).

3 Results and discussion

3.1 Immersion test results

Fig.1 shows the microstructure of AZ31 alloy that consists of primary α-Mg phase and AlMn phase. AlMn locates at the grain boundary and in the matrix.

Figs.2−4 show the surface morphologies of AZ31 alloy immerged in solution B for 1, 2 and 4 h, respectively.
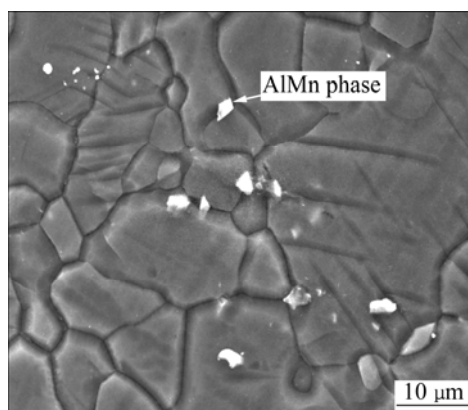
Fig.1 Microstructure of AZ31 alloy
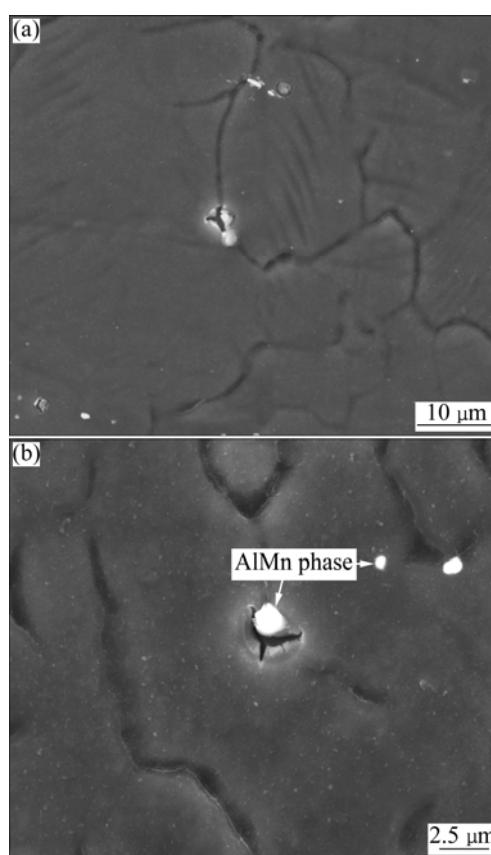
Fig.2 Surface morphologies of AZ31 alloy immerged in solution B for 1 h

the immersion time is 1 h, the cracks could be observed around AlMn particles that locate at the grain boundary. With increasing immersion time, the cracks grow bigger. At the same time, more and more AlMn particles locating at the grain boundary drop off. However, the AlMn particles in the matrix still exist. After immersion for 4 h, pitting corrosion happens.

AlMn phase plays an important role in the initiation process of localized corrosion. According to Ref.[10], AlMn phase acted as cathode like β phase, even the AlMn phase was inerter than β phase in the solution
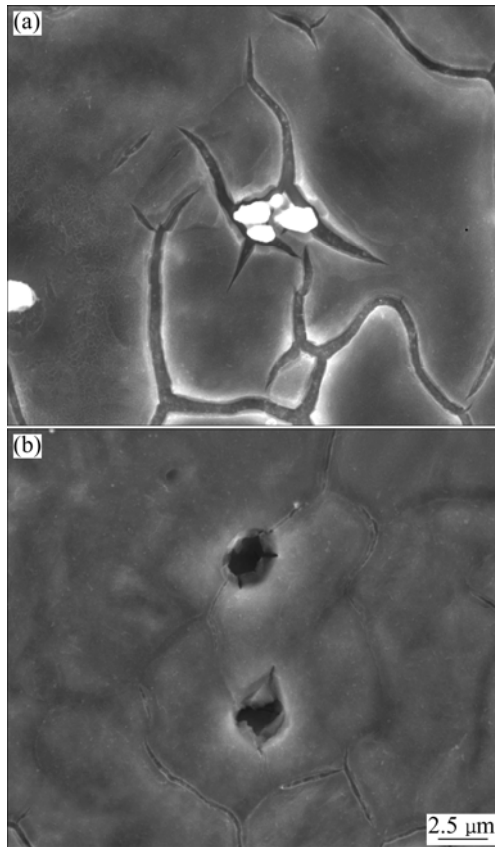
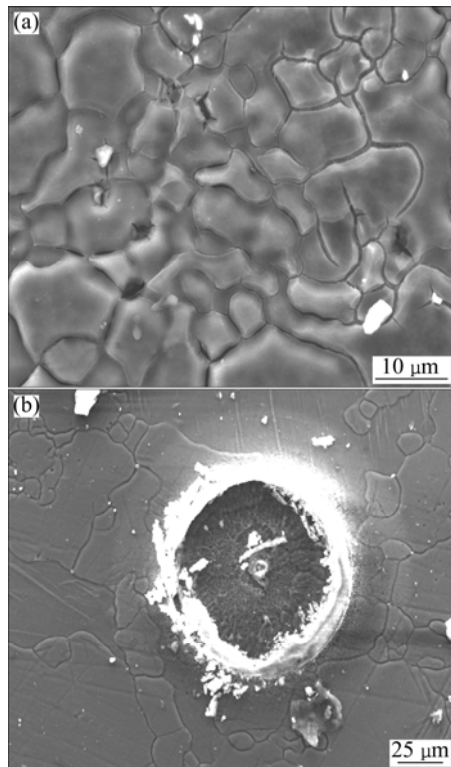**Fig.3** Surface morphologies of AM50 alloy immerged in solution B for 2 h

Fig.4 Surface morphologies of AM50 alloy immerged in solution B for 4 h

containing Cl⁻ ion. The concentration of Al had a great influence on the corrosion of Mg matrix[5], due to the formation of a passive Al_2O_3 film on the surface of matrix which could prevent the corrosion to some degree. Thus, the corrosion could easily happen around AlMn phase where the concentration of Al was lower. Additionally, the grain boundary of AZ31 has more tendencies to be corroded in the corrosive medium than the matrix due to the effect of deformation.

3.2 EIS results for immersion experiments

Fig.5 shows the Nyquist diagrams for AZ31 in solutions A, B and C when the immersion time is 1 h. The plots consist of one high-frequency (HF) capacitive loop, one medium-frequency (MF) capacitive loop and one low-frequency (LF) inductive loop. Fig.6 shows the equivalent circuit of AZ31 immerged in solution A, B, C for 1 h. R_1 in parallel with the capacity C_1 represents the characters of double layer on Mg substrate. C_2 in parallel with R_2 that in series with diffusion impedance Z_w indicates the characters of $Mg(OH)_2$ film on Mg substrate. The inductance L in series with charge transfer resistance R_3 is induced by Mg^+. The dimension of HF capacitive loops decreased with the increase of the concentration of Cl⁻ in Fig.5, which meant that the corrosion resistance of AZ31 decreased with the increase of the concentration of Cl⁻. The dimension of HF capacitive loops decreases with increasing concentration of Cl⁻ ion as shown in Fig.5, which means that the corrosion resistance of AZ31 decreases with increasing the concentration of Cl⁻ ion.
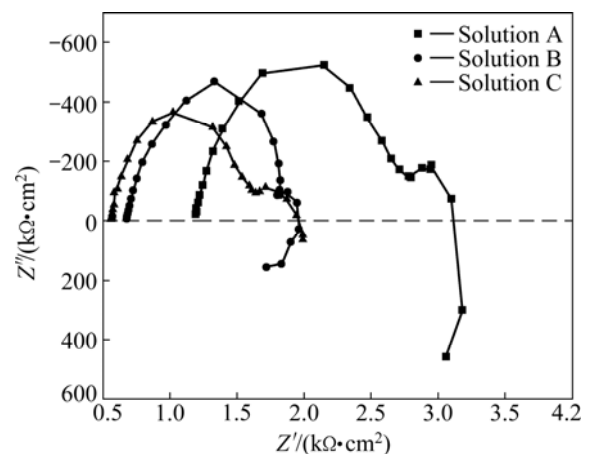

Fig.5 Nyquist diagrams of AZ31 alloy in solutions A, B, C for 1 h

Fig.7 shows the fitting values of C_1 and R_1. The values of C_1 increase with increasing concentration of Cl⁻ ion. According to SONG et al[3] and CHEN et al[11], C_1 increases with decreasing surface film coverage. So, in SAR solution with higher concentration of Cl⁻ ion, the $Mg(OH)_2$ film is destroyed more severely. R_1 decreases

with increasing concentration of Cl⁻ ion. The reactions occurring at the interface are accelerated with the existence of Cl⁻ ion[4].

Fig.8 shows the Nyquist diagrams for AZ31 in solutions A, B and C when immersion time is 24 h. The plots consist of one capacitive loop and one inductive loop. The inductive loop presents that the pitting corrosion has already happened on the electrode surface.
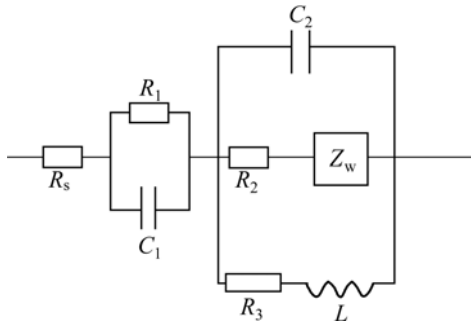

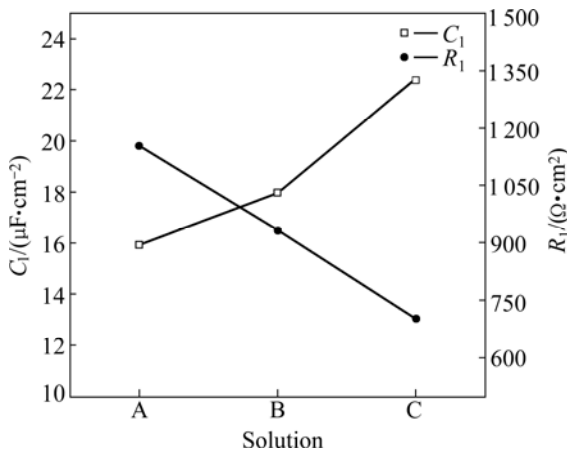**Fig.6** Equivalent circuit of AZ31 immerged in solutions A, B, C for 1 h

Fig.7 Values of C_1 and R_1 in equivalent circuit of AZ31 alloy immersed in solution A, B and C for 1 h
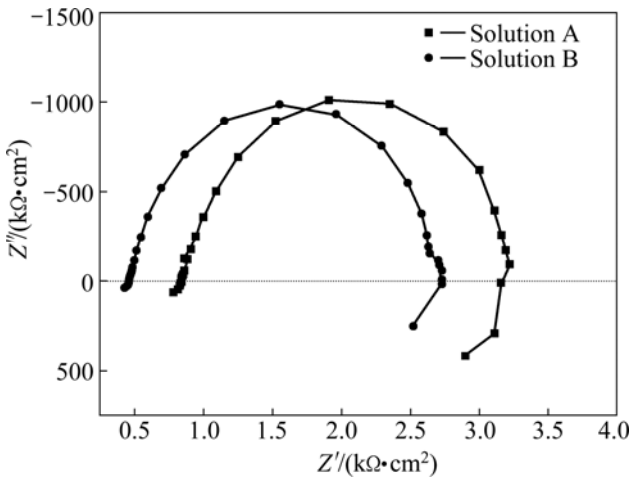

Fig.8 Nyquist diagrams of AZ31 alloy in solutions A and B for 24 h

Thus, the concentration of Cl⁻ is not the main affecting factor inducing pitting corrosion.

3.3 Polarization curves of AZ31 in different concentration of Cl⁻ SAR

Fig.9 shows the polarization curves of AZ31 in SAR solution with different times of concentration of Cl⁻ ion without immersion. It can be seen that φ_{corr} keeps constant, and this means that the thermodynamic stability of AZ31 alloy is not changed greatly with increasing concentration of Cl⁻ ion in SAR solution[14]. The anode branch and cathode branch of polarization curves correspond to the anodic dissolution and hydrogen evolution for magnesium alloy. The anode and cathode branch of polarization curves shift towards right, which means that the rate of anodic dissolution and hydrogen evolution increase with increasing concentration of Cl⁻ ion. This indicates that the corrosion of magnesium alloy in SAR solution is controlled by the rate of anodic dissolution and hydrogen evolution[14]. So, the corrosion rate of AZ31 alloy increases with increasing concentration of Cl⁻ ion.
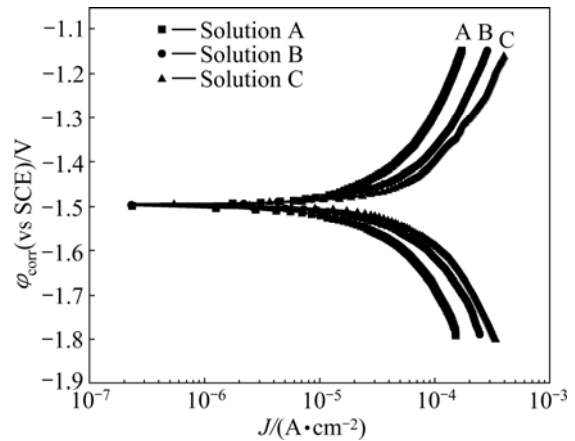

Fig.9 Polarization curves for AZ31 in solutions A, B and C without immersion

4 Conclusions

1) At the initial stage of immersion, the matrix around AlMn phases locating at the grain boundary are corroded more severely, and the AlMn particles in this region drop off with increasing immersion time.

2) Pitting corrosion happens for AZ31 in SAR solution, and it happens around the AlMn phases locating at the grain boundary.

3) Cl⁻ ion accelerates the corrosion rate of AZ31 magnesium alloy, but it is not the main affecting factor inducing pitting corrosion.

4) The corrosion of AZ31 magnesium alloy in SAR solution is controlled by the rate of anodic dissolution

and hydrogen evolution, and the corrosion rate of AZ31 increases with increasing concentration of Cl⁻ ion.

References

[1]   LINDSTROM R, JOHANSSON L G, THOMPSON G E, SKELDON P, SVENSSON J E. Corrosion of magnesium in humid air [J]. Corrosion Science, 2004, 46(5): 1141−1158.

[2]   CHEN J, DONG J H, WANG J Q, HAN E H, KE W. Effect of magnesium hydride on the corrosion behavior of an AZ91 magnesium alloy in sodium chloride solution [J]. Corrosion Science, 2008, 50: 3610−3614.

[3]   SONG G L, JOHANNESSON B, HAPUGPDA S, STJOHN D. Galvanic corrosion of magnesium alloy AZ91D in contact with aluminium alloy, steel and zinc [J]. Corrosion Science, 2004, 46: 955−977.

[4]   TUNOLD R, HOLTAN H, BERGE M H, LASSON A, HANSEN R S. The corrosion of magnesium in aqueous solution containing chloride ions [J]. Corrosion Science, 1977, 17(4): 353−365.

[5]   SONG G L, ATRENS A, WU X L, ZHANG B. Corrosion behaviour of AZ10, AZ490 and AZ80 in sodium chloride [J]. Corrosion Science, 1998, 40(10): 1769−1791.

[6]   CHEN J, WANG J Q, HAN E H, KE W. In situ observation of crack initiation and propagation of the charged magnesium alloy under cyclic wet-dry conditions [J]. Corrosion Science, 2008, 50: 2338−2341.

[7]   CHEN J, WANG J Q, HAN E H, KE W. In situ observation of formation and spreading of micro-droplets on magnesium and its alloy under cyclic wet-dry conditions [J]. Corrosion Science, 2007, 49: 1625−1634.

[8]   ZHOU W Q, SHAN D Y, HAN E H, KE W. Initial corrosion behavior of AZ91 magnesium alloy in simulating acid rain under wet-dry cyclic condition [J]. Transactions of Nonferrous Metals Society of China, 2008, 18: 334−338.

[9]   ASTM STP 1238. Cyclic cabinet corrosion testing [S].

[10]   JONSON M, THIERRY D, LEBOZEC N. The influence of microstructure on the corrosion behavior of AZ91D studied by scanning Kelvin probe force microscopy and scanning Kelvin probe [J]. Corrosion Science, 2006, 48: 1193−1208.

[11]   CHEN J, WANG J Q, HAN E H, DONG J H, KE W. AC impedance spectroscopy study of the corrosion behavior of an AZ91 magnesium alloy in 0.1M sodium sulfate solution [J]. Electrochim Acta, 2007, 52(9): 3299−3309.

[12]   CAO C N. Corrosion electrochemistry [M]. Beijing: Chemical and Industrial Press, 1994. (in Chinese)

(Edited by LONG Huai-zhong)